

# Multimodal analysis of prompt neutron spectra for $^{238}\text{Pu}(\text{sf})$ , $^{240}\text{Pu}(\text{sf})$ , $^{242}\text{Pu}(\text{sf})$ and $^{239}\text{Pu}(\text{n}_{\text{th}},\text{f})$

Takaaki Ohsawa <sup>a</sup>, Tetsuo Horiguchi <sup>b</sup>, Miki Mitsuhashi <sup>a,1</sup>

<sup>a</sup> Department of Nuclear Engineering, Faculty of Science and Technology, Kinki University, 3-4-1 Kowakae, Higashi-osaka 577-8502 Japan

<sup>b</sup> Atomic Energy Research Institute, Kinki University, 3-4-1 Kowakae, Higashi-osaka 577-8502 Japan

Received 13 July 1999; received in revised form 5 October 1999; accepted 1 November 1999

## Abstract

The prompt neutron spectra for  $^{238}\text{Pu}(\text{sf})$ ,  $^{240}\text{Pu}(\text{sf})$ ,  $^{242}\text{Pu}(\text{sf})$  and  $^{239}\text{Pu}(\text{n}_{\text{th}},\text{f})$  were calculated with the modified Madland–Nix model with consideration to the multimodal nature of the fission process. The spectra of neutrons for each mode (Standard-I, -II, -III) were calculated independently and the total spectra were synthesized. The partial spectra for the three modes were found to be considerably different from each other. Different mode branching ratios resulted in different total spectra for the three even-mass spontaneously fissioning isotopes. Comparison of spectra for  $^{240}\text{Pu}(\text{sf})$  and  $^{239}\text{Pu}(\text{n}_{\text{th}},\text{f})$ , for which the fissioning nucleus is the same, revealed that the total spectra were harder for  $^{239}\text{Pu}(\text{n}_{\text{th}},\text{f})$  due to the higher excitation energy of the fissioning nucleus. The calculated total spectra well represented the experimental data. © 2000 Elsevier Science B.V. All rights reserved.

PACS: 21.10.Ma; 24.10.-i; 24.75.+i; 25.85.Ec; 27.90.+b

Keywords: NUCLEAR REACTIONS;  $^{238}\text{Pu}(\text{sf})$ ;  $^{240}\text{Pu}(\text{sf})$ ;  $^{242}\text{Pu}(\text{sf})$ ;  $^{239}\text{Pu}(\text{n}_{\text{th}},\text{f})$ ; Calculated prompt neutron spectra; Multimodal fission model

## 1. Introduction

Schillebeeckx et al. [1] showed from experiments that the mass and total kinetic energy (TKE) distributions of fission fragments of plutonium isotopes show a systematic change, which was interpreted as being due to systematic changes in the branching ratios to Standard-I and Standard-II modes in the fission process (Fig. 1). This fact, in turn, was considered as supporting evidence that the multimodal concept of fission [2] was a

<sup>1</sup> Present address: Graduate School of Energy Science, Kyoto University, Yoshida, Sakyo-ku, Kyoto 606-8501 Japan.

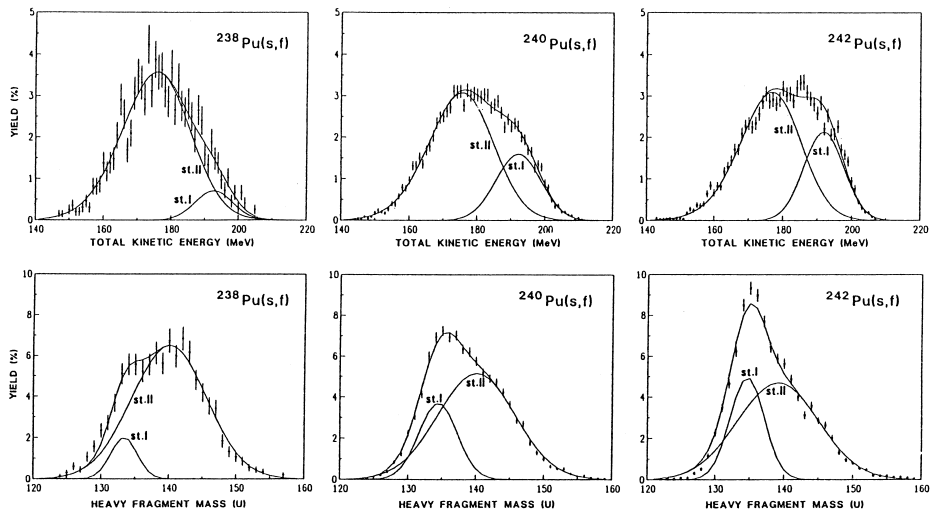


Fig. 1. Mass and total kinetic energy distributions for  $^{238}\text{Pu}(\text{sf})$ ,  $^{240}\text{Pu}(\text{sf})$  and  $^{242}\text{Pu}(\text{sf})$  deconvoluted into Standard-I and Standard-II fission modes (taken from Ref. [1]).

valid tool, at least in an approximate sense, of interpreting the mass and TKE distributions of fission fragments of many fissioning systems.

One of the crucial points in calculating the prompt neutron spectrum is how to treat the neutron emission from a wide variety of fission fragments with a wide variety of excitation energy. A complete Hauser–Feshbach or cascade evaporation calculation of neutron emission from primary fission fragments with distributed excitation energy would be desirable from a theoretical point of view. However, taking into account the entire distribution of fission fragments with a distribution of charge and kinetic energy of fission fragments requires a tremendous amount of data and/or assumptions as well as calculational efforts. In order to solve these complexities, the present authors [3] proposed to introduce the idea of multimodal fission to the calculation with the Madland–Nix model [4] (abbreviated as MN model hereafter). Thus we divided the entire fission fragments into a few groups, each represented by modal average masses and TKE, and calculated the prompt neutron spectrum for each mode (called ‘modal spectrum’ in this paper) independently using available empirical data. The total neutron spectrum was obtained by superposition of the modal spectra weighted with respective probability of occurrence multiplied with the prompt neutron multiplicity for each mode. Application of this methodology [3] to the evaluation of prompt neutron spectra for  $^{237}\text{Np}(\text{n},\text{f})$  for incident energies 0.3 to 5.5 MeV revealed that (a) a systematic change of hardness was observed in partial neutron spectra for different fission modes, and consequently, (b) a change in the modal branching ratio in the fission process led to a change in prompt neutron spectra, resulting in a more sensitive dependence on the incident neutron energy.

In the present study, an attempt is made to apply the multimodal analysis of prompt neutron spectra to spontaneous fission of even-mass plutonium isotopes of  $^{238}\text{Pu}$ ,  $^{240}\text{Pu}$ ,  $^{242}\text{Pu}$ , and to thermal-neutron-induced fission of  $^{239}\text{Pu}$ . Madland [5] published results of calculations of prompt neutron spectra for even-mass isotopes of plutonium using the

experimental data of Wagemans et al. [6] for the mass and TKE distributions of fission fragments. It is interesting to compare the present results where each mode was treated independently and Madland's results where several fission modes were collapsed into a single average fragment pair.

This approach brings about the possibility of understanding the systematic change of the prompt neutron spectra for actinide nuclei in conjunction with the change in the number of modes and in the branching ratios to each fission mode, without too many complications.

## 2. Method

Schillebeeckx et al. [1] found that orderly changes observed in mass and total kinetic energy distributions in  $^{238}\text{Pu}(\text{sf})$ ,  $^{240}\text{Pu}(\text{sf})$ ,  $^{242}\text{Pu}(\text{sf})$  and  $^{239}\text{Pu}(\text{n}_{\text{th}},\text{f})$  could be interpreted as due to a systematic change in the branching ratios to Standard-I (S1), Standard-II (S2) and Standard-III (S3) modes during the fission process according to the mass number of the fissioning nuclei. These data were adopted as the basis of the present analysis.

In the present work, the MN model [3] was used with some modifications. The level density parameters (LDPs) were calculated using the Ignatyuk model [7] instead of using the conventional formula of the type  $a = A/C$ , where  $a$  is the LDP,  $A$  the mass number of the fission fragment,  $C$  an adjustable constant ranging from 8 to 11 (the constant  $C = 10$  was used for Pu isotopes in Ref. [5]), because the Ignatyuk model with shell effects was found to yield a better representation of the LDPs for fission fragments, especially in the mass region near shell closure [8].

Another modification was that different number of neutrons emitted from light (LF) and heavy fragments (HF) was considered. An implicit assumption was made in the original MN model that an equal number of neutrons was emitted from the two fragments. However, it has been known that more neutrons are emitted from LF than from HF in low-energy-neutron-induced fission and this tendency is inverted at higher incident energies for  $^{235}\text{U}(\text{n},\text{f})$  and  $^{237}\text{Np}(\text{n},\text{f})$  [9,10]. For  $^{239}\text{Pu}(\text{n}_{\text{th}},\text{f})$ , the measured average numbers of neutrons emitted from LF and HF were  $\nu_{\text{L}} = 1.56$  and  $\nu_{\text{H}} = 1.36$ , respectively [11]. This is an important fact to notice because the laboratory-system spectra of neutrons emitted from LF are considerably harder than those from HF because of the larger velocity of LF (the measured average velocities are  $v_{\text{L}} = 1.41$  cm/ns and  $v_{\text{H}} = 1.02$  cm/ns for  $^{239}\text{Pu}(\text{n}_{\text{th}},\text{f})$  [12]). This was confirmed in our calculation (Fig. 2) and also in an experiment [11]. We therefore used the following formula:

$$\chi_i(E_n) = [\nu_{\text{iL}} \chi_{\text{iL}}(E_n) + \nu_{\text{iH}} \chi_{\text{iH}}(E_n)] / (\nu_{\text{iL}} + \nu_{\text{iH}}) \quad (1)$$

to synthesize the modal spectra  $\chi_i(E_n)$  from laboratory-system spectra  $\chi_{\text{iL}}(E_n)$ ,  $\chi_{\text{iH}}(E_n)$  of the two fragments, where the subscript  $i$  stands for a fission mode ( $i = \text{S1}, \text{S2}$  or  $\text{S3}$ ).

The multimodal model assumes that the mass distributions of fission fragments are represented as a sum of several pairs of Gaussian functions, each pair corresponding to a fission mode. Applying the prescription of the MN model to each mode, we were able to obtain the prompt neutron spectrum for each mode. The optical model potential of

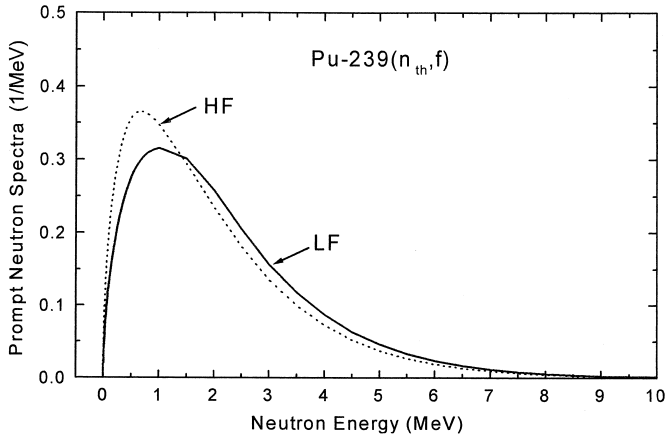


Fig. 2. Comparison of calculated spectra of prompt neutrons emitted from light and heavy fragments in the laboratory system.

Becchetti and Greenlees [13] was used to generate the inverse reaction cross sections for the fission fragments.

### 3. Results

#### 3.1. Basic data for $^{238}\text{Pu}(sf)$ , $^{240}\text{Pu}(sf)$ , $^{242}\text{Pu}(sf)$ and $^{239}\text{Pu}(n_{th},f)$

- (a) *Fragment mass distributions:* The pre-neutron-emission fragment mass distributions were decomposed into four Gaussian functions corresponding to S1- and S2-modes for even-mass isotopes, and six Gaussians with inclusion of the S3-mode for  $^{239}\text{Pu}(n_{th},f)$  [1]. It was observed that, as the mass number of the fissioning nucleus increased, the contribution of the S1-mode (associated with the spherical 82N shell) increased, while that of the S2-mode (deformed 88N subshell) decreased, that of the S3-mode (50N shell and 97N subshell; identified only in  $^{239}\text{Pu}(n_{th},f)$ ) remaining small.
- (b) *Total kinetic energy:* The average TKE of fragments was found to be larger by  $\sim 17$  MeV for the S1- than for the S2-mode (see Table 1), reflecting the difference in the charge-center distance between the two fragments at scission for the two modes [1,2]. The trend of the average TKE for Pu isotopes different from the systematics by Viola et al. [14] and Unik et al. [15] as a function of the Coulomb parameter was also interpreted in terms of the multimodal model [1].
- (c) *Prompt neutron multiplicity:* The total average prompt neutron multiplicity  $\nu_i$  for mode  $i$  was obtained from the calculations of Fan et al. [16] when available, and from calculations by the present authors. It was assumed in these calculations that the precision shape parameters for (sf) of even isotopes were the same as that for  $^{239}\text{Pu}(n_{th},f)$ ; this approximation is justified by the fact that the central masses for S1- and S2-modes for even isotopes stay close to those for

Table 1

Branching ratios and energy partition in  $^{238}\text{Pu}(\text{sf})$ ,  $^{240}\text{Pu}(\text{sf})$ ,  $^{242}\text{Pu}(\text{sf})$  and  $^{239}\text{Pu}(\text{n}_{\text{th}},\text{f})$ . The data of the mode branching ratio and TKE were taken from Schillebeeckx et al. [1]

Quantity	Modes	$^{238}\text{Pu}(\text{sf})$	$^{240}\text{Pu}(\text{sf})$	$^{242}\text{Pu}(\text{sf})$	$^{239}\text{Pu}(\text{n}_{\text{th}},\text{f})$
Branching ratio	S1	9.7%	26.2%	30.7%	24.8%
$w_i$	S2	90.3%	73.8%	69.3%	74.2%
	S3	—	—	—	1.0%
	Average fragments	$^{105}\text{Mo}$ , $^{133}\text{Te}$	$^{106}\text{Mo}$ , $^{134}\text{Te}$	$^{107}\text{Mo}$ , $^{135}\text{Te}$	$^{105}\text{Mo}$ , $^{135}\text{Te}$
$E_R$ (MeV)	S2	$^{98}\text{Y}$ , $^{140}\text{Cs}$	$^{99}\text{Y}$ , $^{141}\text{Cs}$	$^{103}\text{Zr}$ , $^{139}\text{Xe}$	$^{99}\text{Y}$ , $^{141}\text{Cs}$
	S3	—	—	—	$^{83}\text{As}$ , $^{157}\text{Pm}$
	S1	206.11	205.56	205.44	205.40
TKE (MeV)	S2	198.61	199.81	198.37	196.28
	S3	—	—	—	182.12
	S1	192.7	192.2	191.9	190.4
$E^*$ (MeV)	S2	175.1	174.8	175.8	174.2
	S3	—	—	—	164.2
	S1	13.41	13.36	13.54	21.53
$T_m$ (MeV)	S2	23.51	23.01	22.57	28.61
	S3	—	—	—	24.46
	S1	0.798	0.811	0.803	1.017
$a_L, a_H$ (1/MeV)	S2	1.001	0.990	0.986	1.095
	S3	—	—	—	1.032
	S1	11.23 9.37	11.94 8.29	11.94 9.10	11.24 9.58
$\nu_L, \nu_H$	S2	10.56 12.56	11.19 12.56	11.59 11.84	10.76 13.10
	S3	—	—	—	6.67 16.28
	S1	1.57 0.92	1.49 0.91	1.54 0.77	1.58 0.86
	S2	1.48 1.86	1.51 1.77	1.60 1.50	1.40 1.88
	S3	—	—	—	0.32 2.58

$^{239}\text{Pu}(\text{n}_{\text{th}},\text{f})$ . The  $\nu_i$  values were used to give a weighting to the modal spectrum in constructing the total spectrum with the following formula:

$$\chi_{\text{tot}}(E_n) = \frac{\sum_i w_i \nu_i \chi_i(E_n)}{\sum_i w_i \nu_i}, \quad (2)$$

where  $w_i$  is the branching ratio to mode  $i$ .

- (d) *Total energy release*: The total energy release  $E_R$  was calculated with the TUYU mass formula [17] using the seven-point approximation [4] for each mode. It was found that  $E_R$  was the highest for the S1-mode, because the HF in this mode lay close to the double-magic number region with  $A \cong 132$ .

### 3.2. Comparison of modal spectra in fission of plutonium isotopes

The calculated modal and total spectra for  $^{238}\text{Pu}(\text{sf})$ ,  $^{240}\text{Pu}(\text{sf})$ ,  $^{242}\text{Pu}(\text{sf})$  are compared in Figs. 3a–c and those for  $^{239}\text{Pu}(\text{n}_{\text{th}},\text{f})$  is shown in Fig. 4. The energy partition for the two cases are summarized in Table 1. It was observed that the S1-modal spectrum was softer than that for the S2-mode for all the cases analyzed. From Table 1

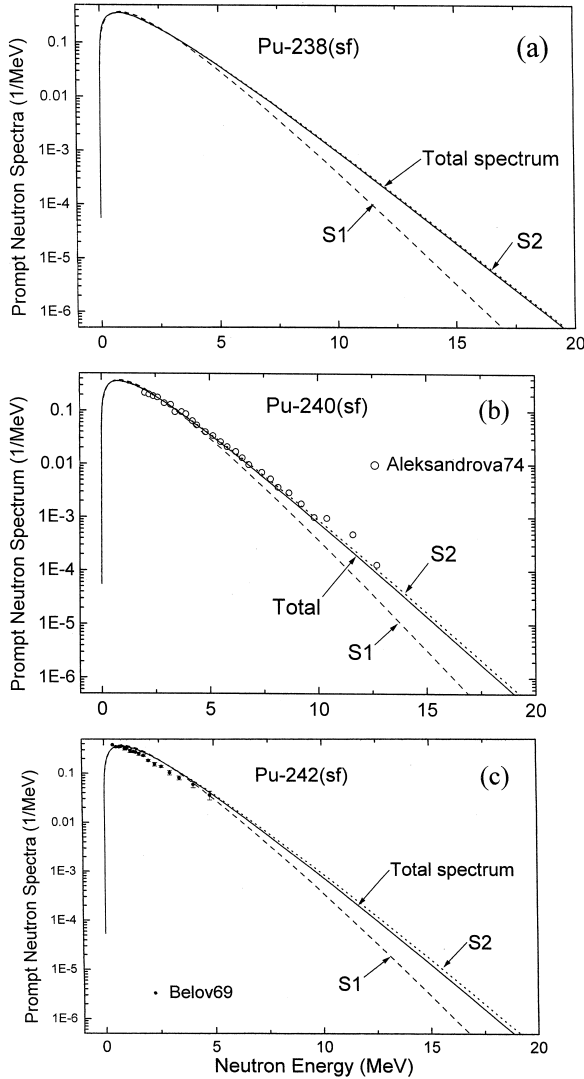


Fig. 3. Modal and total spectra of prompt neutrons in  $^{238}\text{Pu}(\text{sf})$ ,  $^{240}\text{Pu}(\text{sf})$  and  $^{242}\text{Pu}(\text{sf})$ . Experimental data were taken from Aleksandrova et al. [20] for  $^{240}\text{Pu}(\text{sf})$  and from Belov et al. [21] for  $^{242}\text{Pu}(\text{sf})$ .

we can interpret this as follows: although  $E_R$  is larger for the S1-mode, the TKE is also higher due to small charge-center distance for the S1-mode, so that the total excitation energy  $E^*$  is small; thus the maximum nuclear temperature  $T_m$  is lower for the S1- than for the S2-mode as can be seen from Fig. 5 where the nuclear temperature distribution for  $^{238}\text{Pu}(\text{sf})$  is shown. This tendency is exactly the same as for  $^{237}\text{Np}(\text{n},\text{f})$  in our previous analysis [3].

The results for S3-modal spectra are rather ambiguous, because of the larger uncertainty in associated quantities due to the difficulty in separating a small contribution ( $\sim 1.0\%$ ) from the total. The measured average TKE for S3-mode in  $^{239}\text{Pu}(\text{n}_{\text{th}},\text{f})$  is

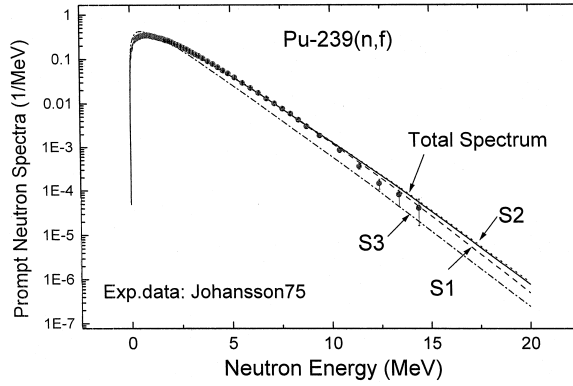


Fig. 4. Modal and total spectra for prompt neutrons in  $^{239}\text{Pu}(n, f)$ . The experimental data were taken from Johansson et al. [22].

164.2 MeV [1], while the corresponding quantity for  $^{237}\text{Np}(n, f)$  is 152.19 MeV at incident energy 5 MeV [18,19]. This prominent difference of 12 MeV in TKE is a reason that the S3-modal spectrum is much softer for  $^{239}\text{Pu}(n, f)$  unlike for  $^{237}\text{Np}(n, f)$ . However, the effect of this difference to the total spectrum is almost negligible due to the small branching to this mode.

Comparing the three spectra in Fig. 3 we see that the total spectrum is determined by combination of the two components S1 and S2. For  $^{238}\text{Pu}(sf)$ , the S2-mode (with harder spectrum) accounts for 90.3% of the total fission process, thus the resulting total spectrum is hardest among the three isotopes. In contrast, for  $^{242}\text{Pu}(sf)$ , the branching ratio to the S2-mode decreases down to 69.3%, thus resulting in the softest total spectrum of the three isotopes. The average energies of prompt neutrons are 2.005 MeV, 1.977 MeV, 1.973 MeV for  $^{238}\text{Pu}(sf)$ ,  $^{240}\text{Pu}(sf)$  and  $^{242}\text{Pu}(sf)$ , respectively. This can clearly be seen in Fig. 6, where the four spectra are compared. This should be compared with previous results of calculations by Madland [5] that the softest spectrum is that of

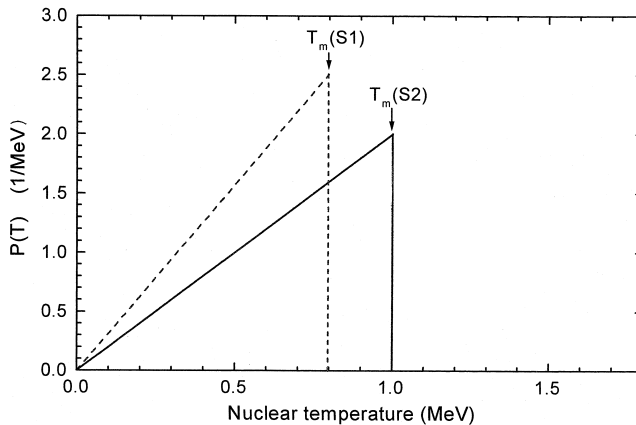


Fig. 5. Nuclear temperature distribution of residual fission fragments for  $^{238}\text{Pu}(sf)$ .

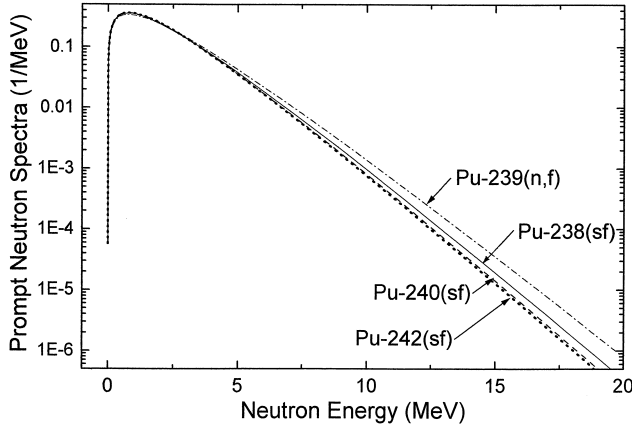


Fig. 6. Comparison of the total prompt neutron spectra for  $^{238}\text{Pu}(\text{sf})$ ,  $^{240}\text{Pu}(\text{sf})$ ,  $^{242}\text{Pu}(\text{sf})$  and  $^{239}\text{Pu}(\text{n}_{\text{th}},\text{f})$ .

$^{242}\text{Pu}(\text{sf})$  whereas the hardest spectrum is that of  $^{240}\text{Pu}(\text{sf})$  among the even-mass plutonium isotopes.

### 3.3. Comparison of the total spectra with experiments

There are only scarce experimental data for (sf) of even-mass isotopes of plutonium. The data available to us [20–22] were plotted in Figs. 3 and 4. It is seen that the present calculation agrees quite well with experiments for  $^{240}\text{Pu}(\text{sf})$  and  $^{239}\text{Pu}(\text{n}_{\text{th}},\text{f})$ . For  $^{242}\text{Pu}(\text{sf})$ , there is a discrepancy between the calculated and experimental data of Belov et al. [21], the shape of the latter being apparently different from those of other isotopes.

### 3.4. Comparison of total spectra for $^{239}\text{Pu}(\text{n}_{\text{th}},\text{f})$ and $^{240}\text{Pu}(\text{sf})$

It is interesting to compare the neutron spectra for  $^{239}\text{Pu}(\text{n}_{\text{th}},\text{f})$  and  $^{240}\text{Pu}(\text{sf})$ , for which the fissioning nucleus is the same. From Table 1 we see that the mode branching ratios,  $E_R$  and TKE are more or less similar for the two cases, the only difference being the addition of the neutron binding energy of 6.534 MeV for  $^{239}\text{Pu}(\text{n}_{\text{th}},\text{f})$ . Thus the harder spectrum of  $^{239}\text{Pu}(\text{n}_{\text{th}},\text{f})$  compared with that for  $^{240}\text{Pu}(\text{sf})$  (see Fig. 6) is exclusively due to the higher total excitation energy of the fission fragments by the amount of the neutron binding energy.

### 3.5. Comparison of single-mode and multimodal calculations

It is also interesting to compare the results of conventional (referred to as “single-mode”) and the multimodal MN model. Fig. 7 compares the results of calculations with the two methods and experimental data [22]. The multimodal calculation is seen to show closer agreement with the experiment. This is because the contribution of the S1-component with softer spectrum softens the total spectrum, though the branching ratio to the S1-mode is only 24.8% for this case. The advantage of the multimodal MN model



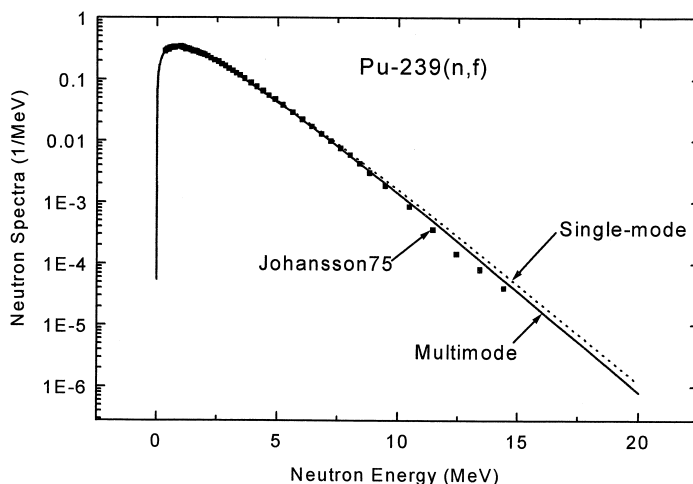


Fig. 7. Comparison of "single-mode" and multimodal MN model calculations for  $^{239}\text{Pu}(n_{th},f)$ .

becomes more evident when it is applied to cases where there are contributions from several different modes or considerable modal changes, as in our previous study [3].

#### 4. Conclusion

A systematic analysis of prompt neutron spectra for plutonium isotopes in terms of the multimodal MN model was made. It was found that the modal spectra associated with S1-mode were softer than those with S2-mode, and that the total spectra were determined by a combination of the two components. The total spectrum for  $^{238}\text{Pu}(sf)$ , for which S2-component accounted for 90.3%, was the hardest, while that for  $^{242}\text{Pu}(sf)$ , for which S2-component accounted for 69.3%, was the softest among the even-mass isotopes.

Recently, new results of analyses of the different Pu isotopes under consideration has been reported by Demattè et al. [23]. Although the branching ratios are not much different except for  $^{242}\text{Pu}(sf)$ , the  $w_{S2}$ -value for  $^{242}\text{Pu}$  is lower (62.7%) than the value (69.3%) used in the present paper. Calculations using the newer value resulted in a softer spectrum, the relative change being +2.8% at 0.75 MeV and -4.1% at 10 MeV. This change makes even more evident the above conclusion that the spectra become softer with the mass number of the Pu isotopes.

The multimodal approach yielded the total spectra that showed better agreement with experiments. This is because the energy partition during the fission process is treated in a realistic way in the multimodal fission model, leading to automatic consideration of the variation of  $T_m$  with the fragment mass regions. Recent advances [24] in the study of systematics of the mode branching ratios in fission will enhance the predictive power of the present method.

## References

- [1] P. Schillebeeckx, C. Wagemans, A.J. Deruytter, R. Barthélémy, Nucl. Phys. A 545 (1992) 623.
- [2] U. Brosa, S. Grossmann, A. Müller, Phys. Rep. 197 (1990) 167.
- [3] T. Ohsawa, T. Horiguchi, H. Hayashi, Nucl. Phys. A 653 (1999) 17.
- [4] D.G. Madland, J.R. Nix, Nucl. Sci. Eng. 81 (1982) 213.
- [5] D.G. Madland, Proc. Int. Conf. on Nuclear Data for Science and Technology, Gatlinburg, 1994 (American Nuclear Society, 1994) Vol. 1, p.532.
- [6] C. Wagemans, P. Schillebeeckx, A. Deruytter, Nucl. Phys. A 502 (1989) 287c.
- [7] A.V. Ignatyuk, Sov. J. Nucl. Phys. 29 (1979) 450.
- [8] T. Ohsawa, T. Shibata, Proc. Int. Conf. on Nuclear Data for Science and Technology, Gatlinburg, 1994 (American Nuclear Society, 1994) Vol. 2, p. 639.
- [9] A.A. Naqvi, F. Käppeler, F. Dickman, Phys. Rev. C 34 (1986) 218.
- [10] R. Müller, A.A. Naqvi, F. Käppeler, F. Dickman, Phys. Rev. C 29 (1984) 885.
- [11] K. Nishio, PhD Dissertation, Kyoto University [in Japanese] (1996) and private communication (1998).
- [12] K. Nishio, Y. Nakagome, I. Kanno, I. Kimura, J. Nucl. Sci. Technol. 32 (1995) 404.
- [13] F.D. Becchetti Jr., G.W. Greenlees, Phys. Rev. 182 (1969) 1190.
- [14] V.E. Viola, K. Kwiatkowski, M. Walker, Phys. Rev. C 31 (1985) 1550.
- [15] L. Unik, J. Gindler, L. Glendenin, K. Flynn, A. Gorski, R. Sjoblom, Proc. Symp. on Physics and Chemistry of Fission, Rochester, 1973 (IAEA, Vienna, 1974) Vol. II, p. 19.
- [16] T.-S. Fan, J.-M. Hu, S.-L. Bao, Nucl. Phys. A 591 (1995) 161.
- [17] T. Tachibana, M. Uno, M. Yamada, S. Yamada, Atomic Data and Nuclear Data Tables 39 (1988) 251.
- [18] P. Siegler, F.-J. Hambsch, S. Oberstedt, J.P. Theobald, Nucl. Phys. A 594 (1995) 45.
- [19] P. Siegler, Ph.D. Dissertation, Technische Hochschule Darmstadt, 1994.
- [20] Z.A. Aleksandrova, V.I. Bol'shov, V.F. Kuznetsov, G.N. Smirenkin, M.Z. Tarasko, Sov. Atomic Energy 36 (1974) 355.
- [21] L.M. Belov, M.V. Blinov, N.M. Kazarinov, A.S. Krivokhatsky, M. Protopopov, Sov. J. Nucl. Phys. 9 (1969) 421.
- [22] I.P. Johansson, B. Holmqvist, T. Wiedling, L. Jeki, Proc. Conf. on Nuclear Cross Sections and Technology, Washington, 1975, Vol. II, p. 572; Numerical data were taken from J.M. Adams, AERE-R8636, Appendix A (1977).
- [23] L. Demattè, C. Wagemans, R. Barthélémy, P. D'Hondt, A. Deruytter, Nucl. Phys. A 617 (1997) 331.
- [24] U. Brosa, H.-H. Knitter, T.S. Fan, J.M. Hu, S.L. Bao, Phys. Rev. C 59 (1999) 767.